SUPPLEMENTARY INFORMATION

SUPPLEMENTARY FIGURES CAPTIONS

Supplementary Figure 1. Single Unit Waveforms and Inter-Spike Interval (ISI) from microwire arrays and characteristics of recorded ensembles. a, Left panel shows 100 waveforms of the task related (tr_i and tr_d) and task unrelated (*tu*) units shown in Fig. 1e (conventions are same). Right panel shows ISI histograms for the corresponding units in the left panel. Scales are same for all waveforms. **b,** Spike-width calculation for identifying putative interneurons and pyramidal cell types. W_1, W_2 and W_3 are widths of three units between the peaks marked by shaded grey lines. **c,** Histogram showing counts of spike widths for each of the three category of units (bin size = 10 μs). **d,** Spike widths for the three categories of units (mean ± s.e.m.). **e,** Relationship between the SWS_{pre} and SWS_{post} firing rates for each of the three category of units. Also plotted is the linear regression fit for tr_d units (m=0.89; R^2=0.89). **f,** Firing rates of the three categories of units in SWS prior to learning the task. **g,** Firing rates of three categories of units in SWS after learning.

Supplementary Figure 2. Tetrode Recordings. a, Example of clusters based on amplitude feature from two channels. **b,** Example of one tetrode with 3 units, each of which had no RPVs (Refractory Period Violations). Shown are the waveforms, autocorrelation, cross-correlation, and linear discriminant analysis (LDA). There was no evidence of a relationship in cross-correlations and clear separation of units according to Fisher's LDA, suggesting over sorting had not occurred. **c**, Respective STA averages from experiments conducted with either tetrode or microelectrode arrays. The distributions were not significantly different (p=0.9579, unpaired t-test).

Supplementary Figure 3. Comparison of the modulation depth and post-learning effects for 'Negative' and 'Positive' weight units. **a,** Comparison of the post-learning firing rates of a single positive-weight unit (tr_d +) and a single negative-weight unit (tr_d -). **b,** Average depth of modulation for tr_d + and tr_d - units. **c,** Distribution of the modulation depths for all tr_d + and tr_d - units (bin size=5%). **d,** Mean STA amplitude change for the respective population of tr_d + and tr_d - units.

Supplementary Figure 4. Changes in STA during task performance. **a,** Top panel compares the STA of a task related (tr_d) unit during early (blue) and late (red) trials during task performance/learning in a single session. This STA is based on 'Beta' band filtered LFP (i.e. 12-40 Hz). In contrast, we did not observe significant changes in other bands (e.g. SWA band, theta, alpha, higher frequencies) as shown in the unfiltered STA beneath it. **b,** This shows the population averages of the change in STA amplitude when comparing early and late trials from robust learning sessions. This indicates a significant drop in locking of spiking to the Beta band for task related units. Reduced locking of units to this frequency is consistent with the broader notion of 'movement-related desynchronization' that is commonly observed with movements[1] or neuroprosthetic control[2]. Interestingly, *tu* units did not display this relationship. * ANOVA test followed by t-test, * $p < 0.0001$.

Supplementary Figure 5. Hypnogram. **a,** Top panel depicts sleep and awake transitions. Bottom panels show the respective LFP activity/EMG activity. **b,** Comparison of SWS duration for all of the pre- and post- robust learning sessions (n=15 sessions, p=0.98, paired t-test).

Supplementary Figure 6. Changes in locking to spindle and ripple frequency bands. **a,** Left panel shows the STA of a tr_d unit in the ripple band (100-300Hz) in SWS_{pre} and SWS_{post}. Right panel illustrates the mean change in STA for the three classes of units. **b**, Left panel shows the STAs in the spindle band (8-20Hz). Right panel shows the mean changes in STAs for the three unit classes.

Supplementary Figure 7. Power-spectral density (PSD) of the pre- and post-LFP during slow-wave sleep. Summary of the changes in the normalized 0.3-3 Hz power for the entire duration of SWS (SWS_{pre}: 2271.42 ± 80.79 s and SWS_{post}: 2189.75 ± 39.54s and, N= 15 sessions, p=0.704)**.**

Supplementary Figure 8. Firing characteristics prior to and after learning. a, Interspike-interval histograms of a task-related unit during SWS_{pre} and SWS_{post}. These were based on spiking that occurred during the SWA negativity. The two distributions are not significantly different from each other (KS test, $p > 0.05$), indicating no significant change in bursting. **b,** Comparison of the ISI distributions for SWS_{pre} and SWS_{post}. Each bar shows the percentage of units that did not experience a significant change in the ISI distribution. **c**, Comparison of the delta wave density in SWS_{pre} and SWS_{post} for robust learning sessions (n=15 sessions, p=0.16).

Supplementary Figure 9. ON/OFF periods across LFP channels. a, Grid shows task related and unrelated units at various sites on the microwire probe. Segments of the SWS_{post} LFP are shown for a variety of electrode recording sites. **b**, Bar plot showing temporal lags (i.e. temporal delay in milliseconds) between OFF periods for channels with tr_d and 'distant' *tu* units (i.e. at least two channels away from a tr_d). **c**, Bar plot showing density of OFF periods in the channels with tr_d and distant *tu* units.

Supplementary Figure 10. Spike-field coherence (SFC) magnitude and phase after learning. a, Plot of the full SFC spectrum as a function of frequency before (blue) and after (red) skill acquisition for a tr_d and *tu* unit (0-20Hz band is shown in Fig 3). **b**, Distribution of phases of tr_d, tr_i and *tu* units are shown in pre and post-SWS in a polar plot. Mean phase of tr_d units is shown in bold blue (before) and red (after) vector. The phases were uniformly distributed and didn't change significantly for each of the comparisons for the three classes of units between SWS_{pre} and SWS_{post}.

Supplementary Figure 11. Averaged cross-correlation histograms (CCH). The mean of the peak-to-tail ratio for each of the three categories (tr_d-tr_d, tr_d-tr_i and tr_d-*tu* neuronal pairs) in their CCHs. *ANOVA, followed by t-test $p<0.0001$.

Supplementary Figure 12. Changes in reactivation strength during awake versus SWS. a, Reactivation strength of the signal component during SWS_{pre}, $Awake_{post}$ (shown in gray in right panel) and SWS_{post}. **b,** Mean population difference histograms of pre- and post- reactivation strengths for the awake and SWS period. In each case the respective histogram of SWS_{pre} was subtracted from the respective awake and SWS_{post} periods. Also shown is the mean population difference curve for poor learning sessions. * $p< 0.05$, Logrank test showed significantly greater reactivation during post sleep. **c,** Event triggered average of reactivation strength centered on the maximum delta wave negativity for SWS_{post} (red) and awake (purple) sessions. **d,** Comparison of the change in event triggered negativity for the $awake_{post}$ and SWS_{post} time periods. The relative reactivation compares the baseline (time less than 0) to the peak * $p < 0.01$ t-test.

Supplementary Figure 13. Task Improvements after sleep. Average time to reward for the 30 best trials during the first BMI training session (i.e. $Block_{1best}$) compared to the beginning of second session ($Block_{2begin}$). * $p<0.05$ paired t-test.

SUPPLEMENTARY TABLE CAPTIONS

Table 1. Details of fifteen robust learning sessions. The '*' denotes sessions which were followed by a second learning session (i.e. Figure 6).

REFERENCES

1. Murthy, V.N. & Fetz, E.E. Coherent 25- to 35-Hz oscillations in the sensorimotor cortex of awake behaving monkeys. *Proc Natl Acad Sci U S A* **89**, 5670-4 (1992).
2. McFarland, D.J., Krusienski, D.J. & Wolpaw, J.R. Brain-computer interface signal processing at the Wadsworth Center: mu and sensorimotor beta rhythms. *Prog Brain Res* **159**, 411-9 (2006).

Supplementary Figure 1

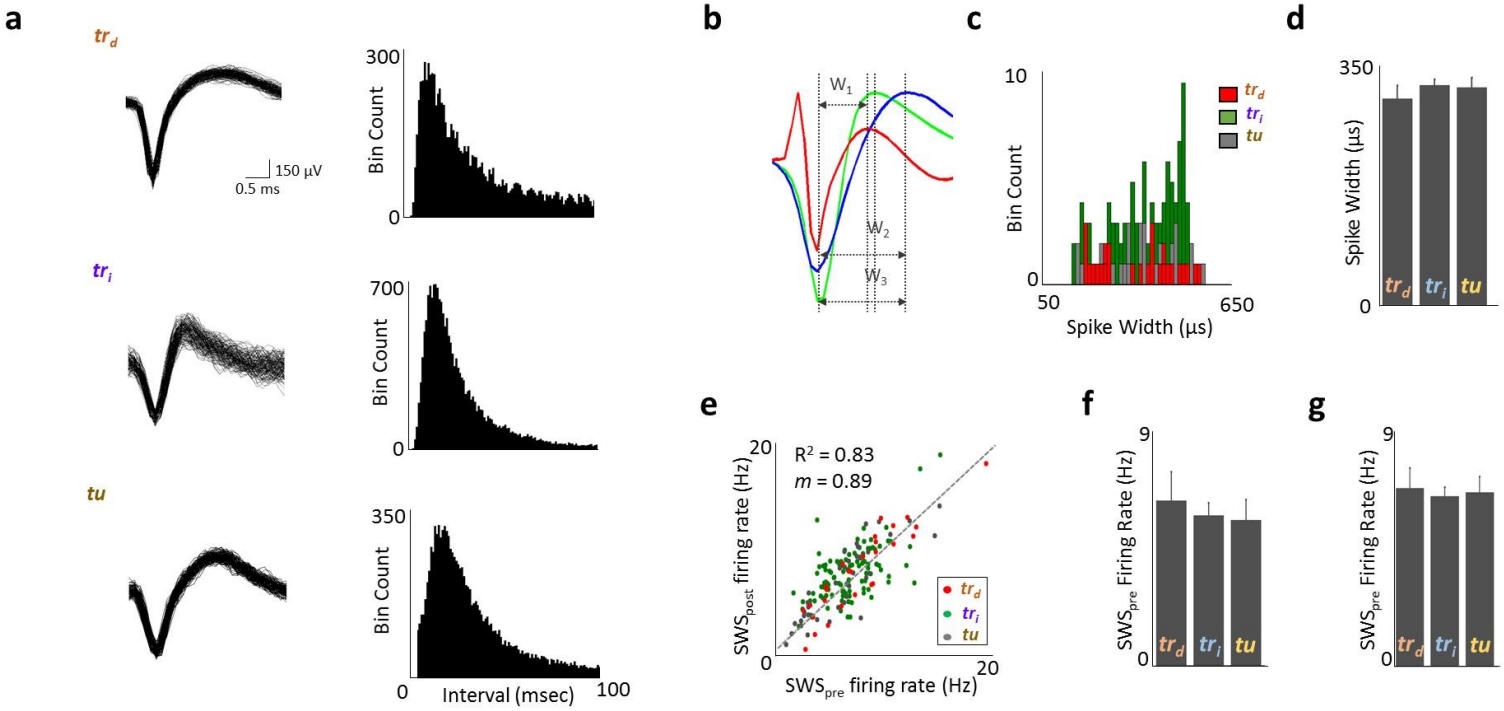

Supplementary Figure 2

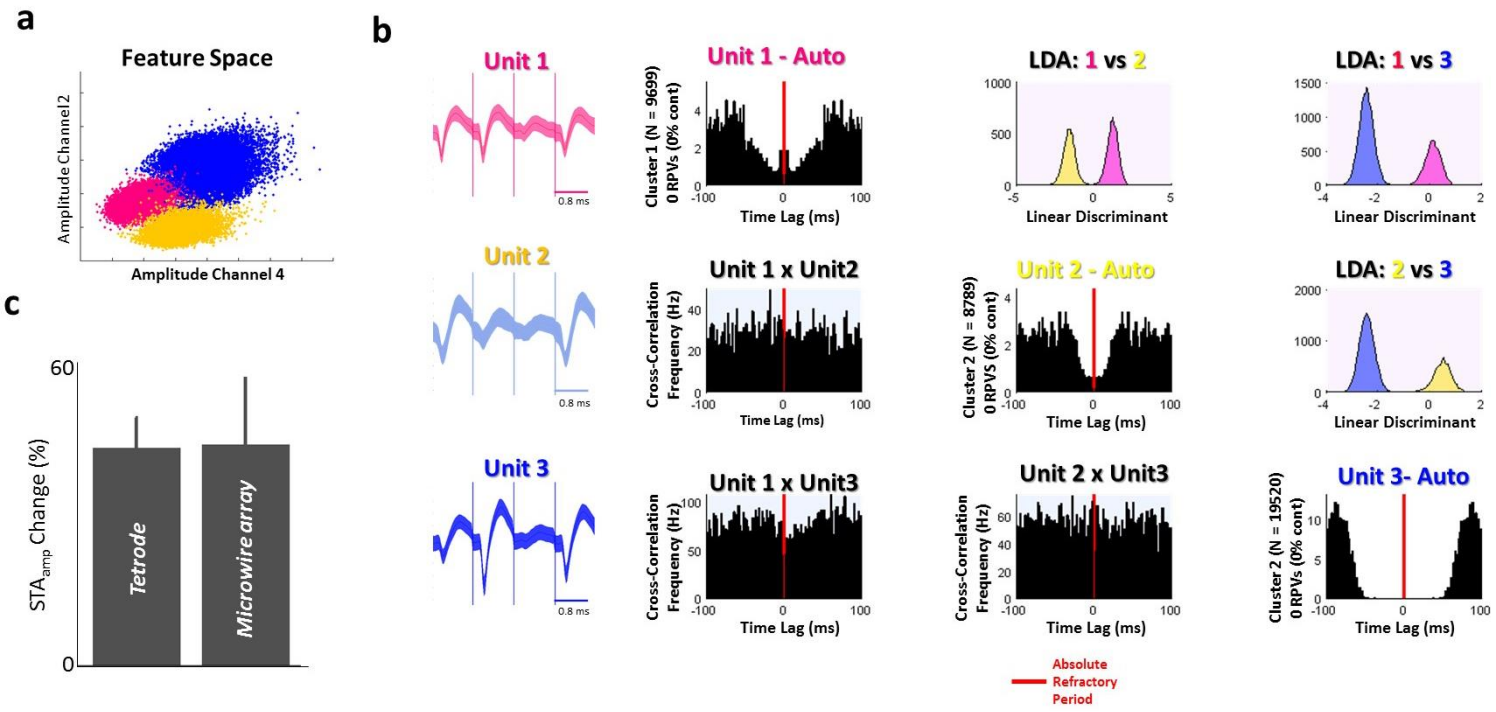

Supplementary Figure 3

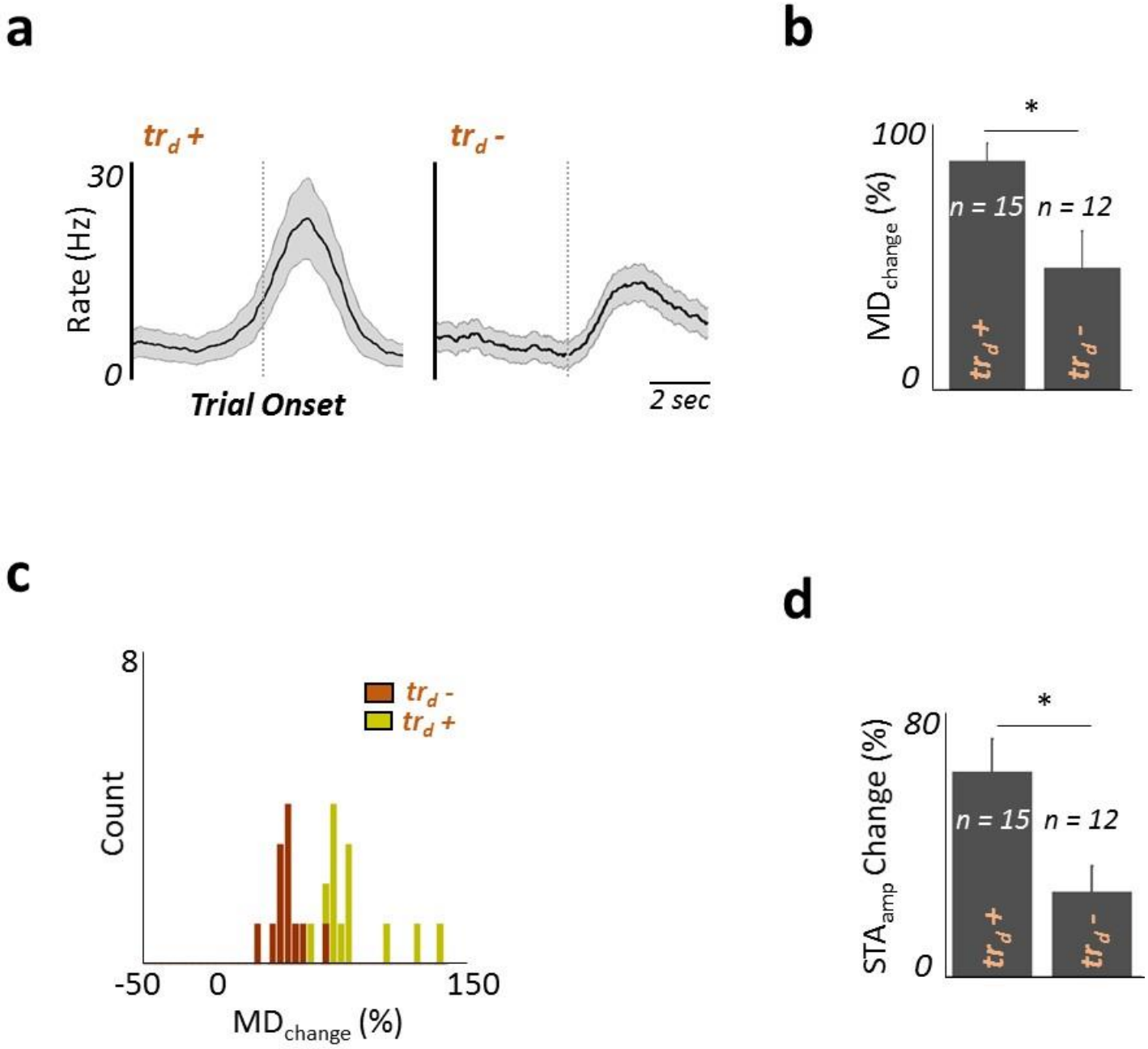

Supplementary Figure 4

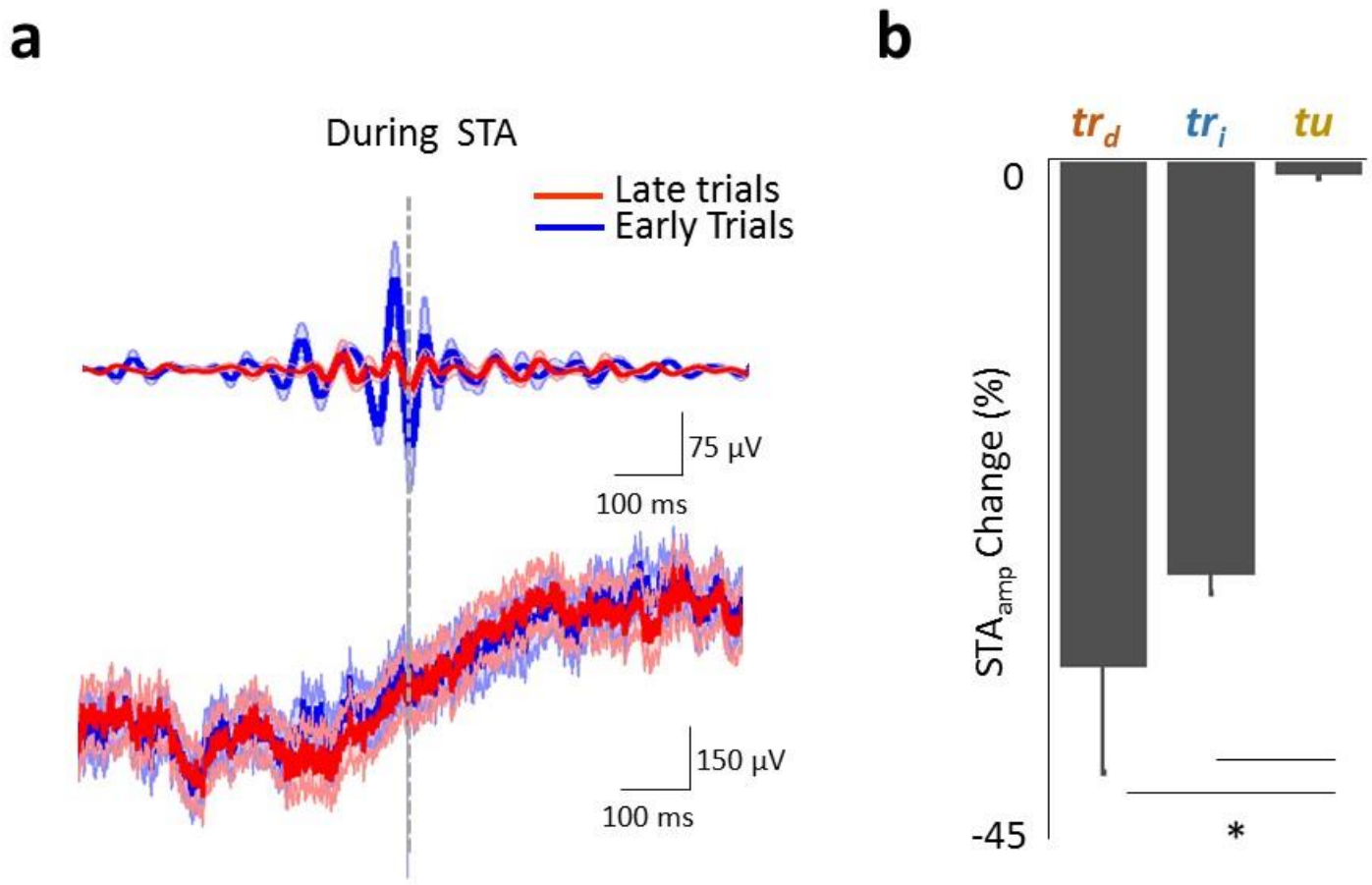

Supplementary Figure 5

a

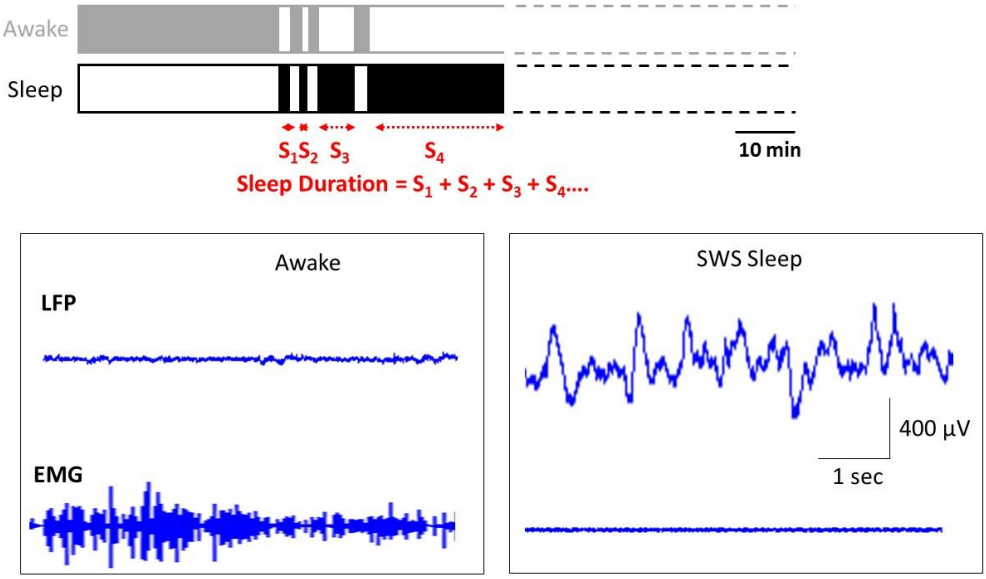

b

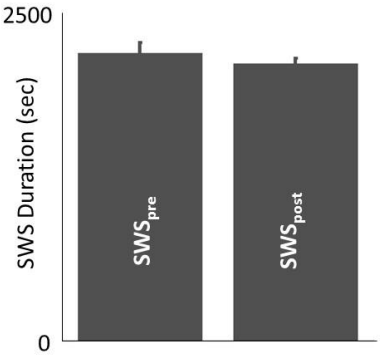

Supplementary Figure 6

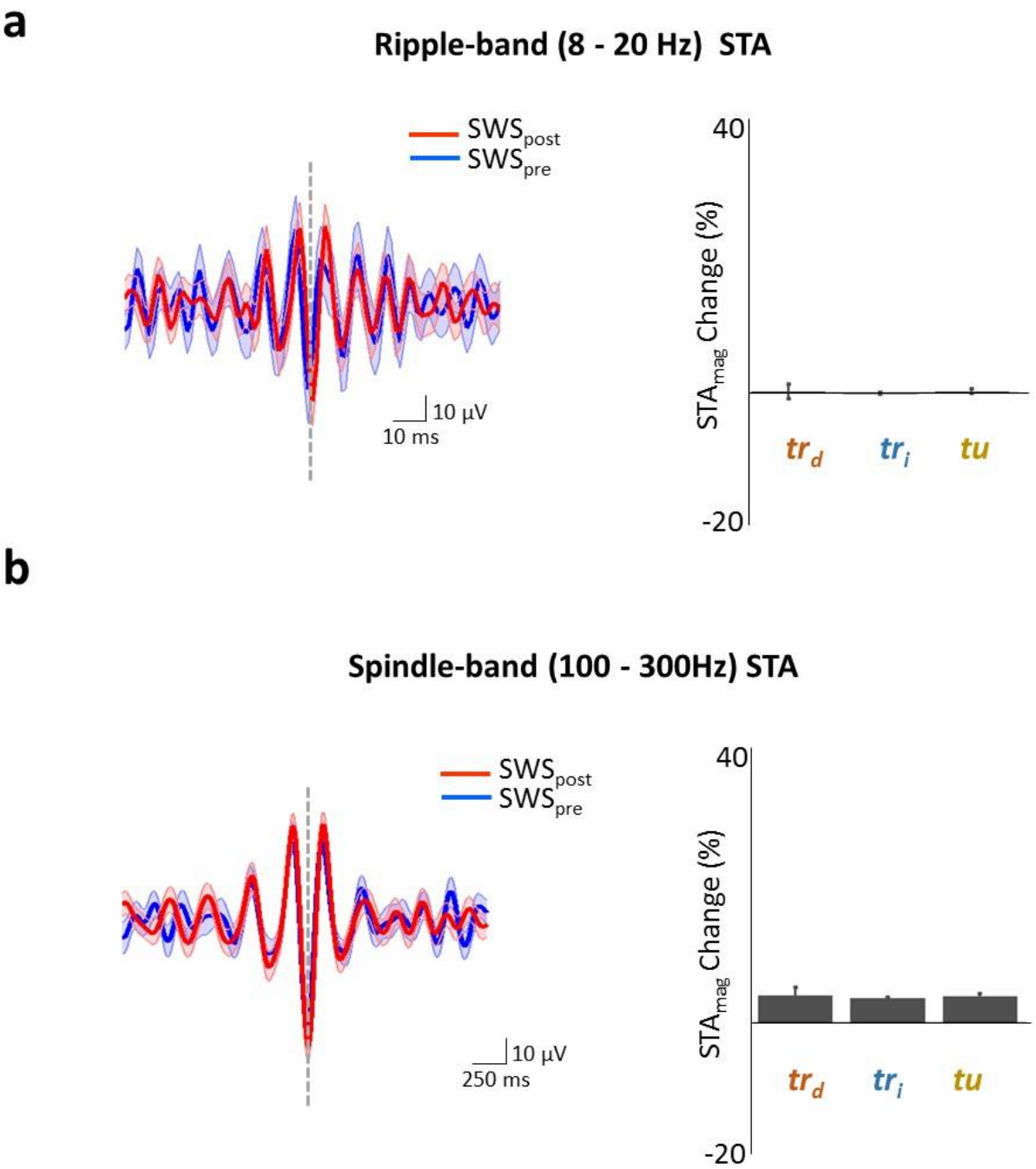

Supplementary Figure 7

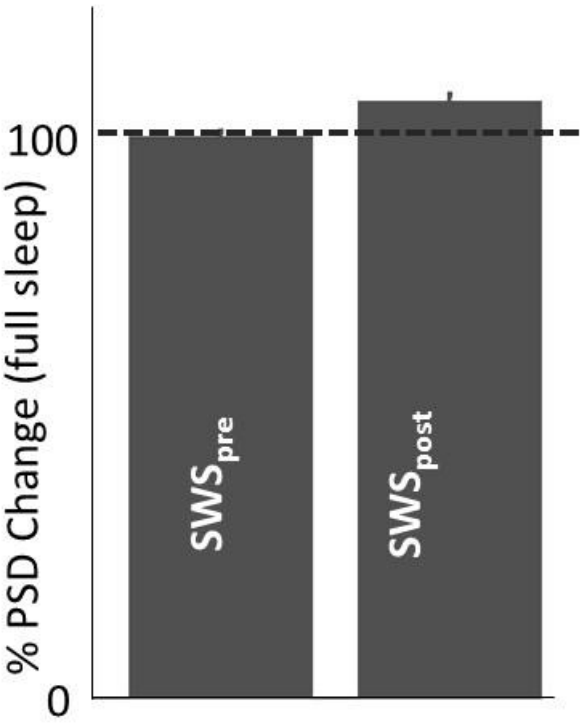

Supplementary Figure 8

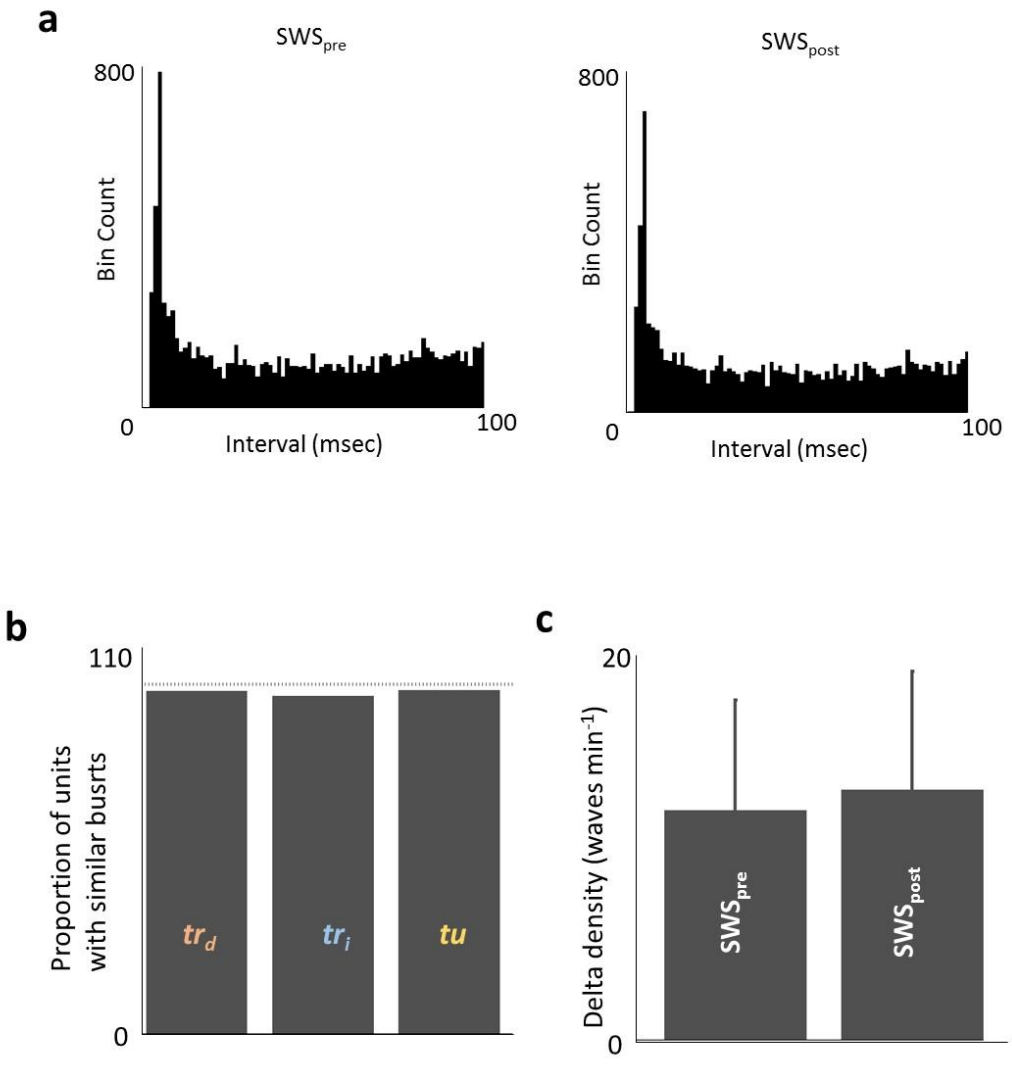

Supplementary Figure 9

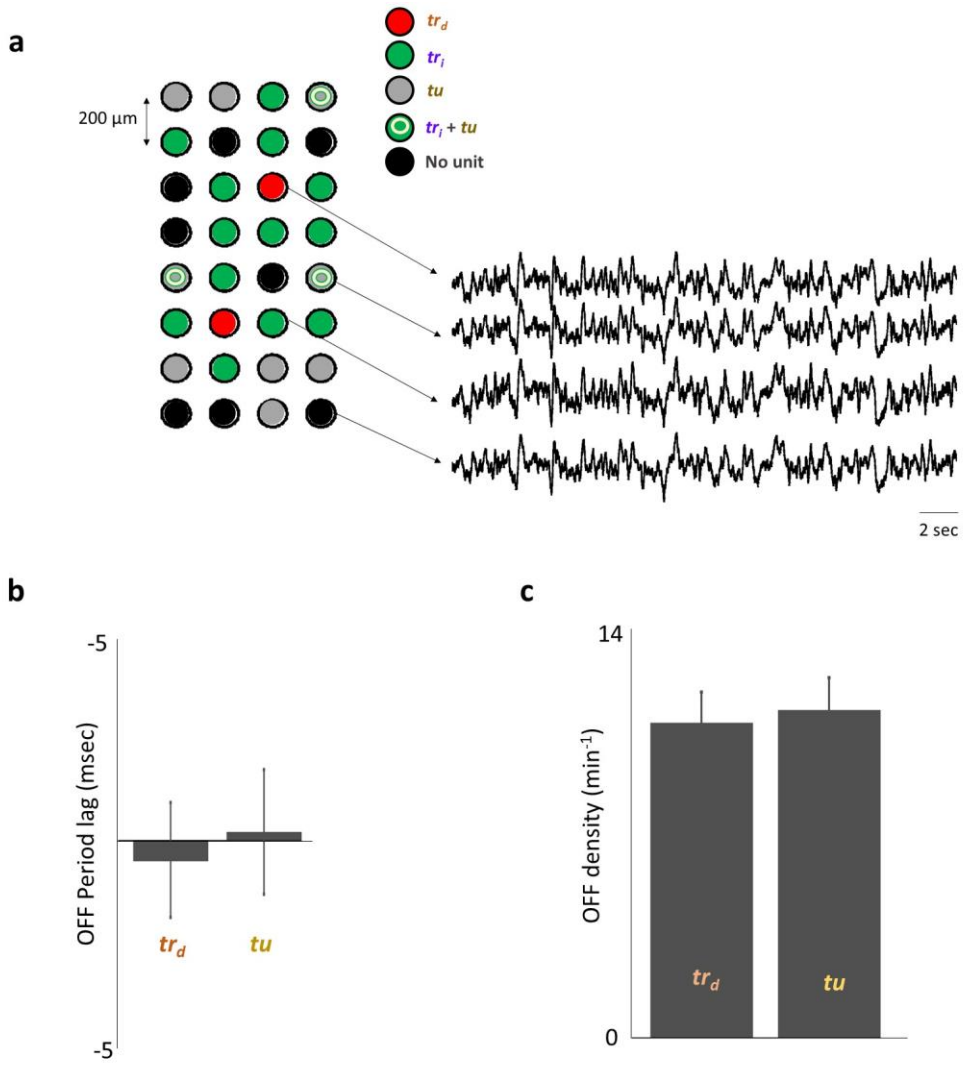

Supplementary Figure 10

a

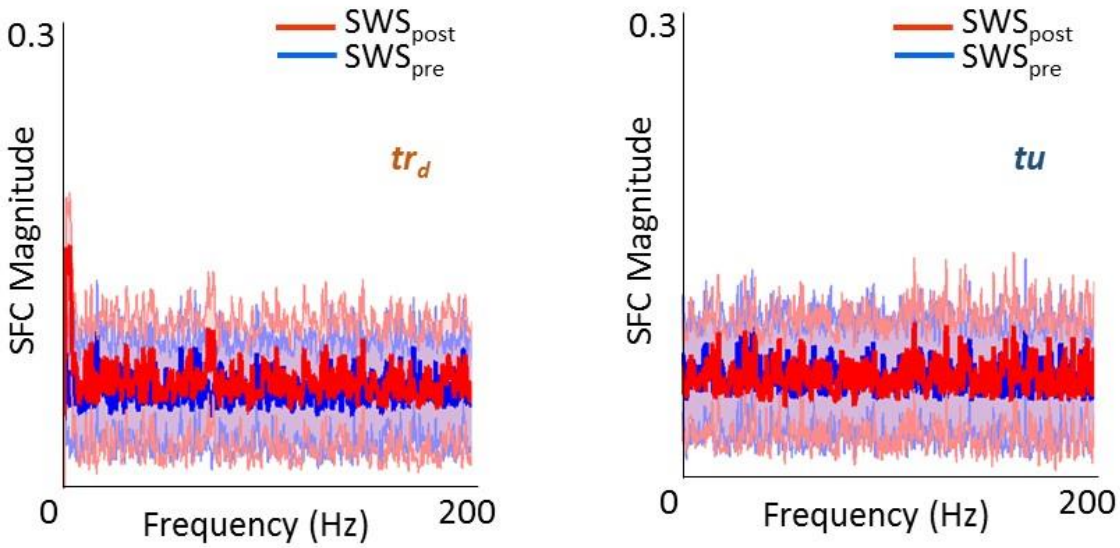

b

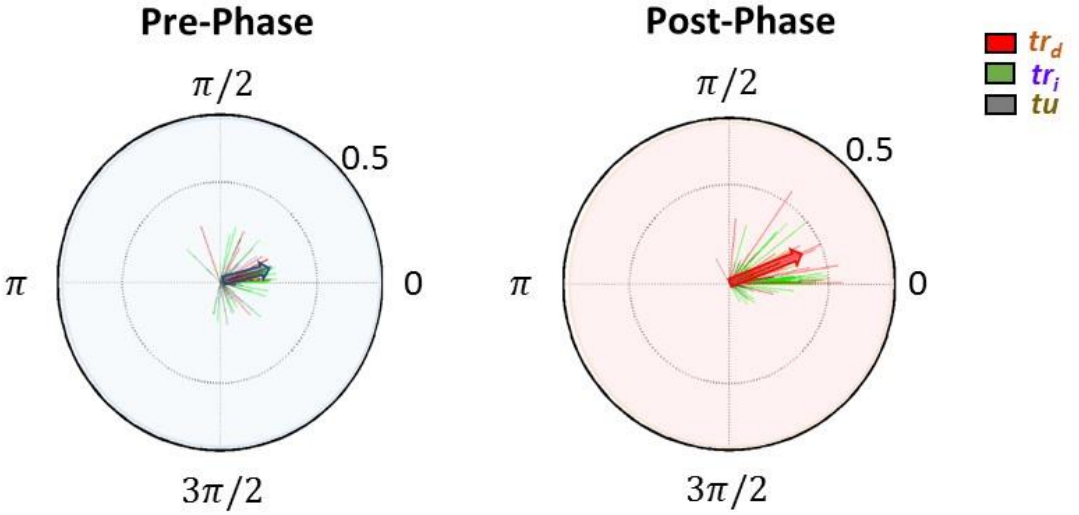

Supplementary Figure 11

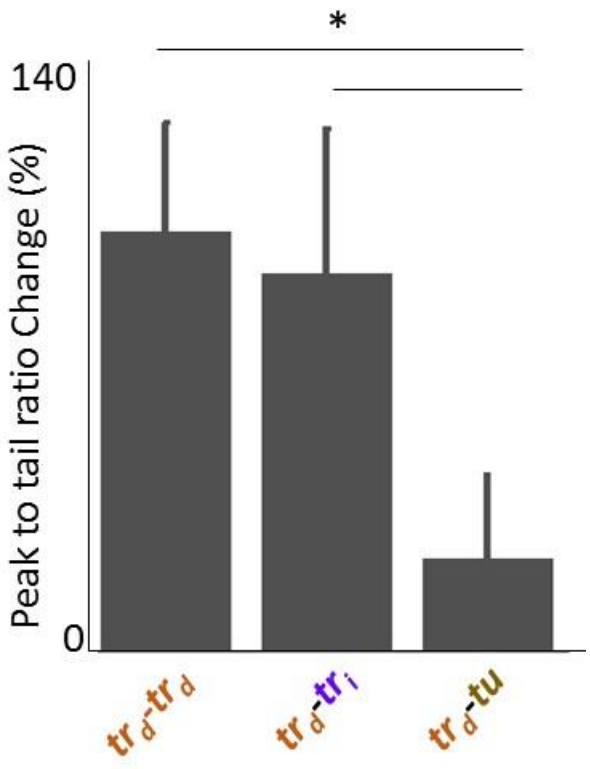

Supplementary Figure 12

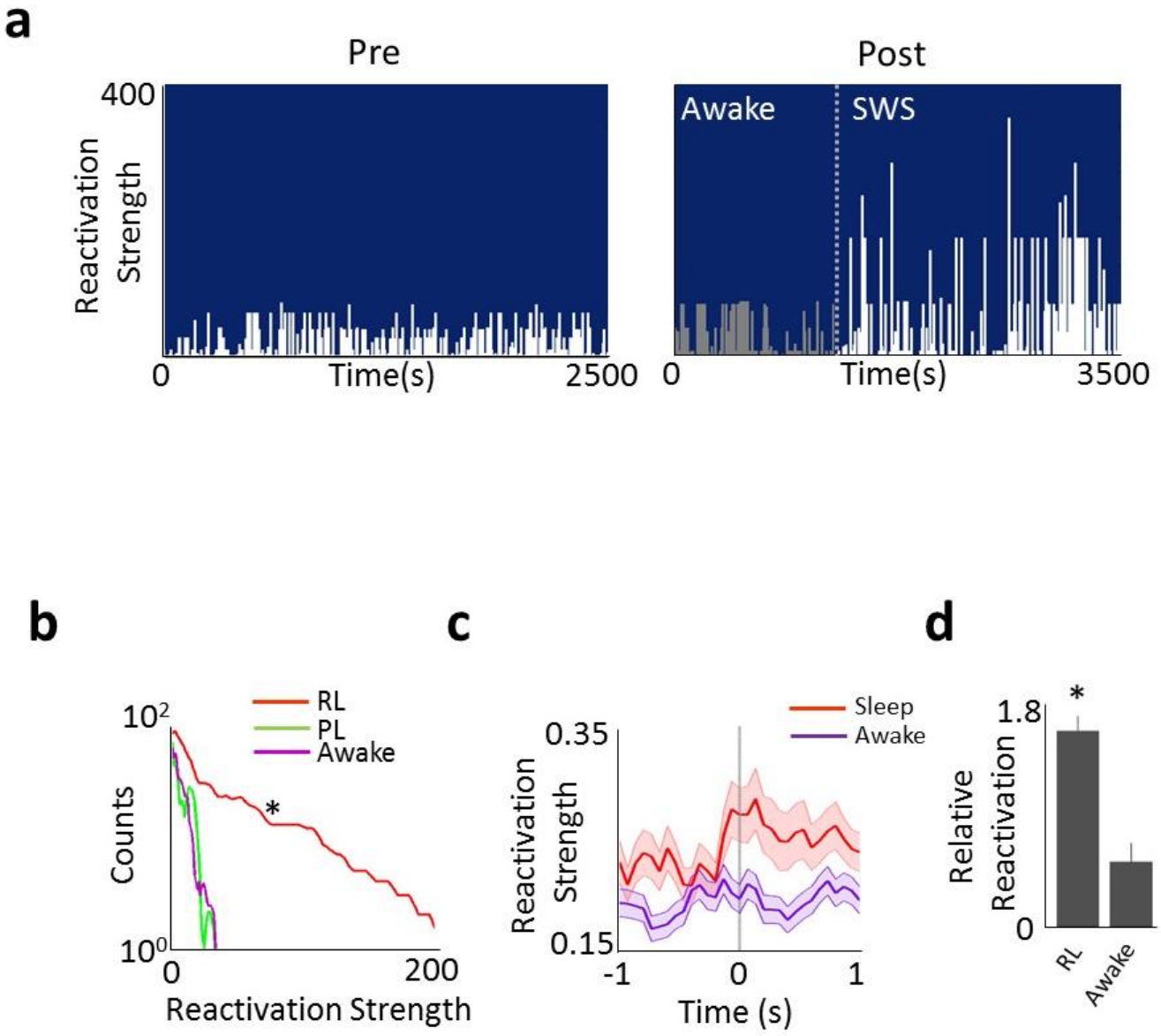

Supplementary Figure 13

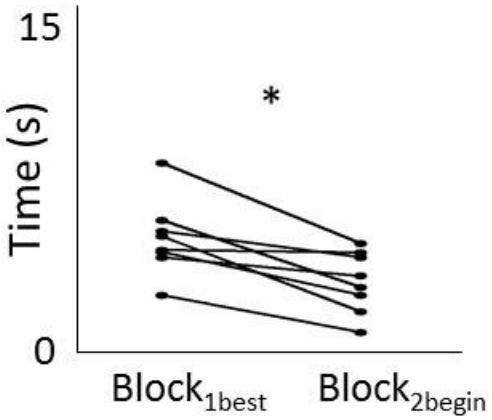

Table 1

Table 1: Table of Units in each session

Session (#)	Rat	Neural Probe	Total no. of cells	tr_d	tr_i	tu
1	Rat 1	MEA	21	2	15	4
2	Rat 1*	MEA	11	2	3	6
3	Rat 2*	MEA	14	2	10	2
4	Rat 2	MEA	24	2	16	6
5	Rat 2*	MEA	16	1	10	5
6	Rat 3*	MEA	10	2	6	2
7	Rat 3	MEA	16	1	9	6
8	Rat 4*	Silicon Probe	6	2	2	2
9	Rat 4	Silicon Probe	6	2	3	1
10	Rat 5*	MEA	10	2	5	3
11	Rat 5*	MEA	10	2	7	1
12	Rat 6*	Silicon Probe	7	2	4	1
13	Rat 6	Silicon Probe	7	2	5	0
14	Rat 6	Silicon Probe	8	1	7	0
15	Rat 6	Silicon Probe	8	2	6	0